CHAPTER-2

LITERATURE REVIEW

2.1 INTRODUCTION

The objective of this chapter is to assemble an extensive review of the various parameters affecting the cavitation flow inside the fuel injector nozzle and its consequent effect on the spray characteristics. The entire review is divided into three sections. In the first section, experimental work has been reviewed for inner nozzle cavitation. In the second part, the analytical and computational fluid dynamic (CFD) models have been reviewed along with the commercial CFD software. The last section covered the coupling methodology between cavitation and spray formation as well as the effect of cavitation on spray formation.

2.2 EXPERIMENTAL STUDY ON CAVITATION FLOW

Several experimental literature works have been published to determine the behaviour of the cavitation flow in the fuel injector nozzle. This experiment helps to understand the structure of cavitation and the two-phase flow pattern. The results of the experimental investigation confirm a significant impact on nozzle efficiency due to cavitation. There is significant progress in the clarification of the structure of cavitation flow inside the nozzle due to studies carried out by several researchers like Bergewerk [8], Nurik [9], Soteriou et al. [10], Chaves et al. [11], Schmidt et al. [12], Arcoumaniset et al. [13], Winklhofer et al. [14], Payri et al. [15], Sou et al. [16], Mauger et al. [17]. These studies throw light on the cavitation phenomena inside nozzles, in particular on the identification of a pattern of quasi-steady-state cavitation flow.

An early pioneer experimental work has been carried out by Begewerk [8] in which he discussed the correlation between fuel injection and cavitation. With the help of the flow visualization technique, the flow through a large size transparent nozzle was observed. The presence of cavitation and hydraulic flip mainly depends upon the cavitation number and has little dependence on the Reynolds number (Re). When the liquid flow entirely separates from the nozzle wall and downstream gas enters the nozzle is known as the hydraulic flip condition. Nurik [9] experimented with a scaled-up transparent nozzle (d=8mm) and observed that cavitation and hydraulic flip depend on cavitation number, nozzle radius, length-to-diameter ratio and pressure difference as shown in Fig.2.1. By adjusting the nozzles' L/d ratios and pressure differential, experiments have been carried out. Based on his research, he has created an empirical association between the nozzle's cavitation characteristics and discharge coefficient. Soteriou et al. [10] experimented with the large-scale transparent injector

nozzle to explore the different flow regimes and the mechanism of its formation inside the nozzle. He emphasizes the effect of hydraulic flips on spray atomization. The flipped nozzle does not experience any wall shear, which leads to poor spray atomization. This condition reduces the turbulence and smooth unbroken liquid jets that come out from the nozzle outlet.

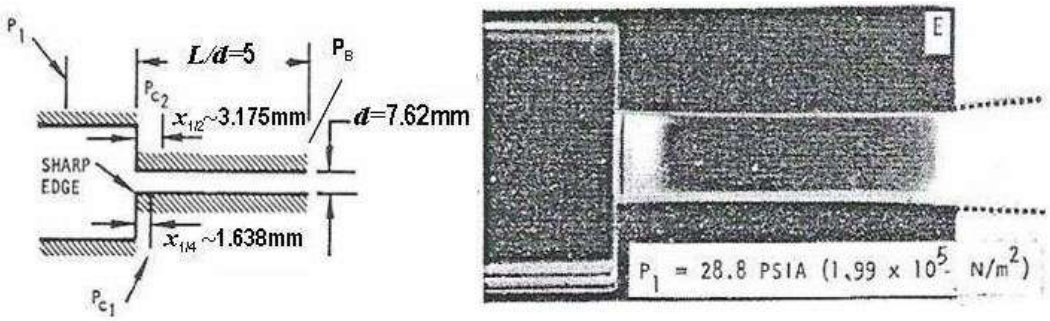

Fig. 2.1 Cavitation observed by Nurik [9] in the transparent nozzle

Although hydraulic flip had never been observed in real scale nozzles with realistic operating conditions. Chaves et al. [11] extended Soteriou et al. [10] work with a small-scale nozzle (d=0.2mm) and injection pressure up to 1000 bar. In his work, he reported super cavitation is different from the hydraulic flip. Super cavitation is referred to when cavitation bubbles reach the nozzle's outlet. In this condition, bubbles collapse at the nozzle exit which is a favourable condition for primary spray breakup. Because there won't be any shear resistance at the nozzle wall, there will be a higher liquid velocity there, which allows the jet to escape the nozzle more quickly. Chaves et al. [11] compared their observations with Soteriou et al. [10] with a large-scale nozzle. Based on these observation Chaves et al. [11] speculated that the bubble has its length scale, and do not scale up in large models. This is due to the lifetime of the cavitation bubble which in the real-size nozzle is similar to the large-size nozzle. Thus, the interaction between the nozzle flow and cavitation phenomena is completely different in large and real-scale nozzles. Cavities were detected on a small size; however, bubbles could be seen on a big scale, indicating that bubbles have their length scales independent of the nozzle's length scale. Although Stoteriou et al. [10] showed that the coefficient of discharge does not depend on the scale of the model. Due to lack of clarity, there is confusion persists to understand the cavitation behaviour and flow pattern at different length scales.

Arcoumanis et al. [13] experimented with large-scale and real-scale acrylic multi-hole injectors. He found that in real-scale experiments there were clear voids were observed and in scaled-up experiments, cloudy bubbles appeared as shown in Fig.2.2. He also found that the cavities are initially clear and become more opaque towards the exit of the real scale nozzle.

The results indicate that the nature of cavitation changes from a large void to a bubbly mixture in scaled-up experiments. However, Schmidt et al. [5] pointed out that the scattering of light from the cavity surfaces may make large void appears as small bubbles. It is complicated to interpret the image which is subjected to multiple scattering of illuminating light. There is no well-established list of non-dimensional parameters that govern the cavitation flow, limiting the scaling of the experiment. Experimental results have shown that the real flow does not always follow the classical scaling theory. The scale effect is caused by liquid quantity, bubble dynamics, geometrical differences due to wall roughness, specific flow regimes, cavitation nuclei etc.

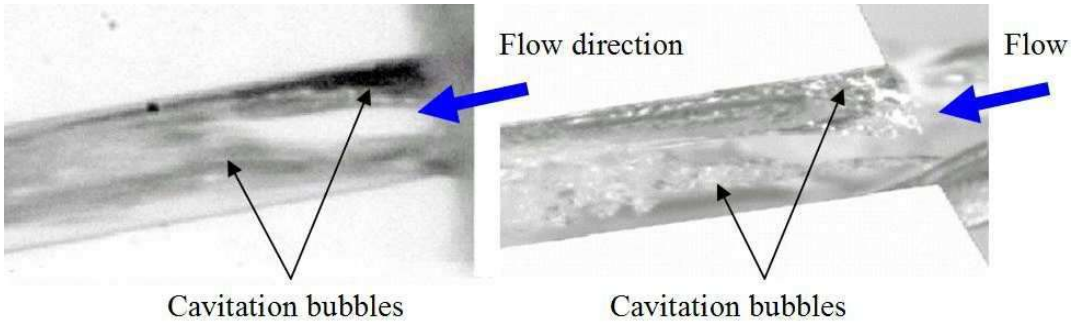

Fig. 2.2 Comparison of hole cavitation for the enlarged (left with CN=5.5) and the real size (right with CN=5.4) nozzle, Arcoumanis et al. [13]

To develop a complete understanding of cavitation flow and its behaviour, qualitative information in a real-size nozzle is essential. However direct observation of cavitation flow in the real condition is difficult due to very small space and time parameters. To observe cavitation in a real-size nozzle, it must be transparent and capable to withstand high injection pressure and choking condition. A good-quality cavitation image will be convenient for the reader as well as for model validation. But as a matter of consequence, only a few experimental works have been found with the above measures. The nozzle flow is visualized by using a shadowgraph technique, schlieren methods, interferometry imaging, Laser doppler velocimetry (LDV), X-ray, computed tomography (CT), X-ray radiography, laser light sheet illumination etc.

Winklhofer et al. [14] experimented with a real-size two-dimensional throttle (transparent rectangular cross-section) working with European diesel fuel as shown in Fig.2.3 (a). A set of optical methods was developed and applied for diagnostics of high-pressure diesel flow at transient conditions by using interferometry imaging shown in Fig. 2.3 (b). They are using three different nozzles named J, U and W throttle with different outlet contractions i.e. 0 %, 5 % & 10 % respectively. They took more than 20-30 backscattered

images of two-phase flow at various pressure differences, and also measured velocity profile with the use of the fluorescence tracking method. Additionally, they employed a distinct colour scheme to distinguish between cavitating, non-cavitating, and foamy (both liquid and gaseous) zones, using blue, red, and yellow hues, respectively. They measured values of the mass flow rate of diesel at the different operating conditions and predicted cavitation inception and choking conditions. They observed that values of mass flow rate in all three types of nozzles (throttle J, U & W) at cavitation inception and choked flow are almost equal even under different operating conditions. The throttle outlet contraction has an influence on pressure distribution within the nozzle and the growth of cavitation regimes. Mauger et al. [17] also experimented with a similar type of transparent two-dimensional micro-channel using test oil as shown in Fig. 2.3 (c). A Schlieren technique has been used to measure density gradient at low pressure, however, the technique does not allow density field reconstruction during high-density gradient. A combination of Schlieren and interferometry imaging techniques has been proposed to reconstruct the density field shown in Fig. 2.3 (d). The outcome demonstrates that the cavitation inception is located relatively far from the inlet corner in the shear layers between the recirculation zones and the main flow.

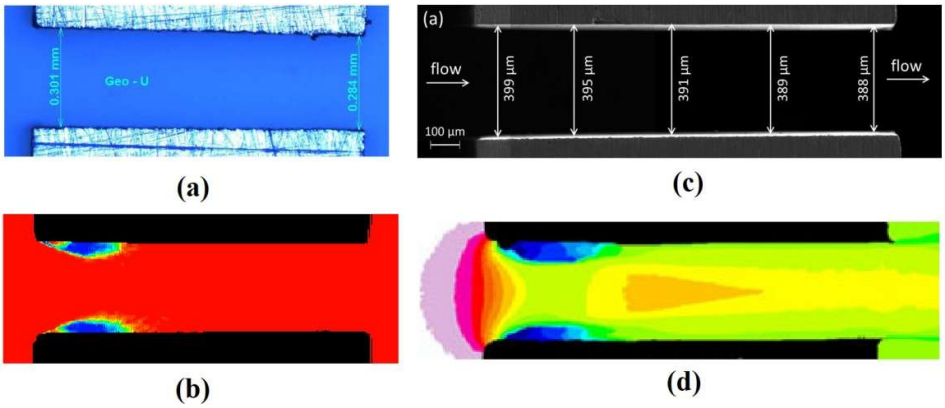

Fig. 2.3 Two-dimensional throttle geometry and cavitation field using interferometry imaging (a, b) Winklhofer et al. [14]and (c, d) Mauger et al. [17]

The physical mechanism behind the initiation, growth, and subsequent bubble collapse of cavitation is investigated using a reduced experimental setup. Results from simplified 2D geometry and simplified working conditions, however, cannot be applied directly to the actual diesel fuel injector nozzle. Few researchers used the real shape and size of the fuel nozzle to study the phenomena of cavitation experimentally. Payri et al. [15] used a single-hole transparent cylindrical nozzle made of fused silica (SiO_2) with an outer diameter of 0.51mm and 1mm in length as shown in Fig. 2.4. Four different fuels n-dodecane, n-

heptane, n-decane & commercial diesel has been used for visualization and parametric study of cavitation flow. The inception of cavitation appears early with low viscous fuel. It is also important to study the effect of geometry shape on the cavitation flow. Cui et al. [18] used a transparent single-hole nozzle to investigate the diameter error, conicality and incline effect, which is commonly found in nozzle geometry. The geometry dimensions were ultra-precisely measured with a micro-hole measuring system. Eleven different shapes of the nozzle geometry (d=0.8 mm to 1.2 mm) were used to visualize the internal flow and their hydraulic characteristics were analysed. They observed that very small differences in geometric structure led to different characteristics of cavitation flow.

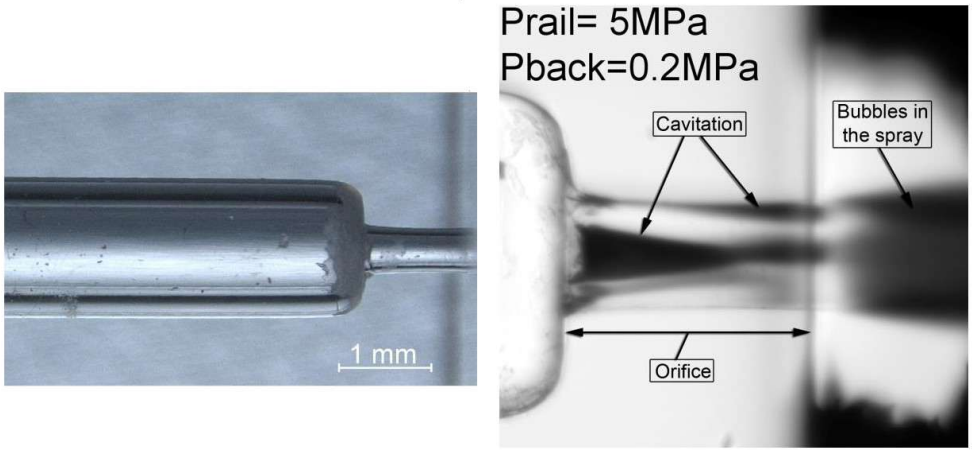

Fig. 2.4 Real size single hole transparent cylindrical nozzle (d=0.51 mm, L=1mm) used by Payri et al. [15]

A transparent nozzle involves the limitation of high injection pressure due to higher material stress generated within the nozzle wall. Transparent materials can be either ductile (acrylic glass) or brittle (sapphire or fused silica). Although acrylic is easily machined, it cannot be used in applications requiring high pressure or temperature. The sapphire or silica is difficult to machine with the conventional machining method. Kirsch et al. [19] proposed the Selective Laser Etching (SLE) method for machining the fused silica. A single-hole transparent nozzle (d=0.3 mm, L=1 mm) has been used to investigate internal nozzle flow and its effect on spray characteristics with a maximum injection pressure of 250 bar as shown in Fig. 2.5. They photographed the transverse waves on the jet surfaces, the mushroom-shaped spray tip, the early reverse flow, and air bubbles inside the nozzle. Experimental work carried out with a real-size nozzle for cavitation flow is summarized in Table 2.1.

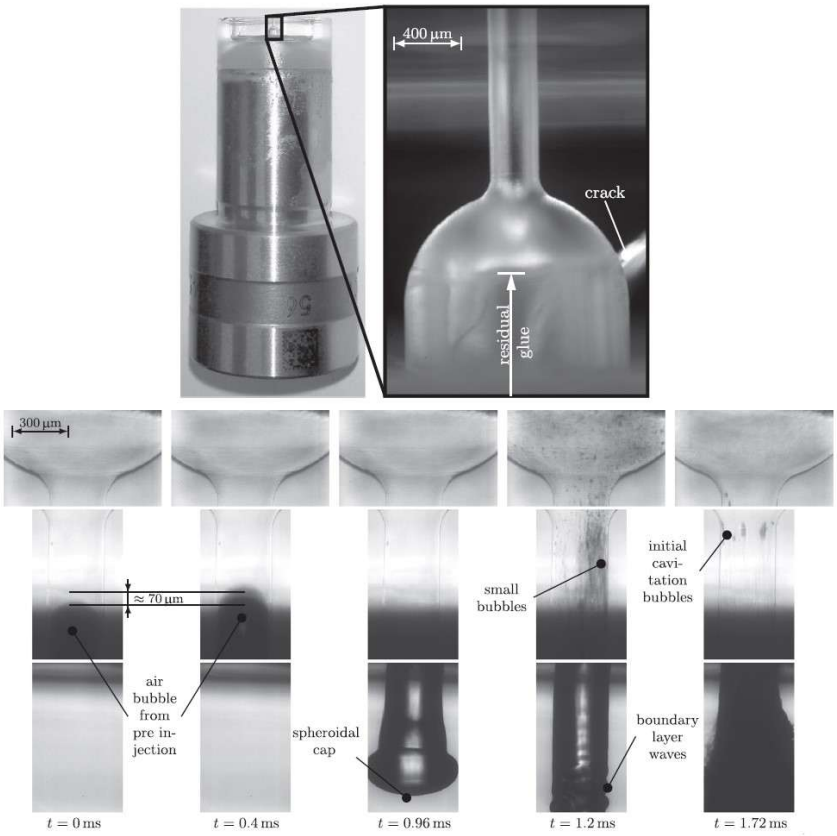

Fig. 2.5 Transparent nozzle (d=0.3 mm, L=1 mm) fabricated by Selective Laser Etching (SLE) method to withstand 250 bar of pressure used by Kirsch et al. [19]

Table 2.1 Summary of Experimental work for cavitation flow with real-size nozzle

Author	Nozzle dimension	Operating pressure	Nozzle material	Visualization technique
Winklhofer et al. [14]	H =0.3 mm, L=1 mm (2D nozzle)	P_{inj}=100 bar P_{back}=20 to 80bar	Steel sheets are sandwiched between a pair of sapphire windows	Highspeed CCD camera with 500ns of exposure time with imaging interferometry
Cyril Mauger et al. [17]	H=0.4mm, L=1.475mm (2D nozzle)	P_{inj}=50bar P_{back}=1 bar	Metal sheets are sandwiched between a pair of glass windows	CCD camera with double pulse laser to capture the image. A shadowgraph technique, the Schlieren method, and interferometry imaging have been used.

Payri et al. [15]	d=0.51mm L=1mm	P_{inj}= 50bar, P_{back}=1 to 15 bar	Fused silica	CCD Camera with 1280X1024 pixels, 1µs of exposure time
Jiwen Cui et al. [18]	d=0.8 to 1.2 mm Five nozzle configu ration	P_{inj}=2 to 10 bar	Transparent nozzles of polymethyl methacrylate	High-speed CCD camera with LED light
Valeri Kirsch et al. [19]	d=0.3 mm, L=1mm	P_{inj}=250 bar, P_{back}=1.5 bar	Fused silica has been fabricated with the Selective Laser Etching (SLE) method.	High-speed CCD camera with 1280X1024 pixels (25000fps) (1µs exposure time)

2.3 COMPUTATIONAL STUDY ON CAVITATION FLOW

2.3.1 One-dimensional modelling of cavitation flow

Nurik[9] experimented by varying pressure difference and L/d ratio with his transparent nozzle. Based on this work he has proposed a one-dimensional theoretical model for predicting the discharge coefficient given below:

$$C_d = C_c\sqrt{K} \tag{2.1}$$

Where$K = \frac{P_{inj}-P_v}{P_{inj}-P_{back}}$, Cavitation parameter, & C_c is the contraction coefficient.

The discharge coefficient (C_d) linearly increases with the cavitation parameter (K) during the cavitation flow. Nurik [9] considers cavitation flow through a sharp edge nozzle. When liquid passes through the minimum cross-sectional area of the nozzle cavitation phenomenon is observed. The values of C_c depend on geometrical parameters, for the sharp edge nozzle it is 0.61 and for the rounded corner, it is between 0.61 to 1. The value of C_c can be calculated with the help of the equation proposed by Weisbach [20].

$$C_c = 0.63 + 0.37\left(\frac{A_2}{A_1}\right)^3 \tag{2.2}$$

Although during non-cavitation flow C_d is not a function of cavitation parameter. Lichtarowicz et al. [21] predicted coefficient of discharge for non-cavitating nozzles by assuming the flow is fully expanded to fill the nozzle. Based on this assumption the discharge coefficient is a constant value of about 0.84.

When the discharge coefficient (C_d) and cavitation parameter (K) plot on the log-log scale, initially C_d increases with K and then remains constant as shown in Fig. 2.6. Nurik [9] confirms this trend through his experiments. Schmidt and Corradini [5] have collected data from similar experimental work and shown them as the graph shown in Fig.2.6. The findings support the 1D model put forth by Nurik [9], and it's also noteworthy that the data lie above the predicted curve.

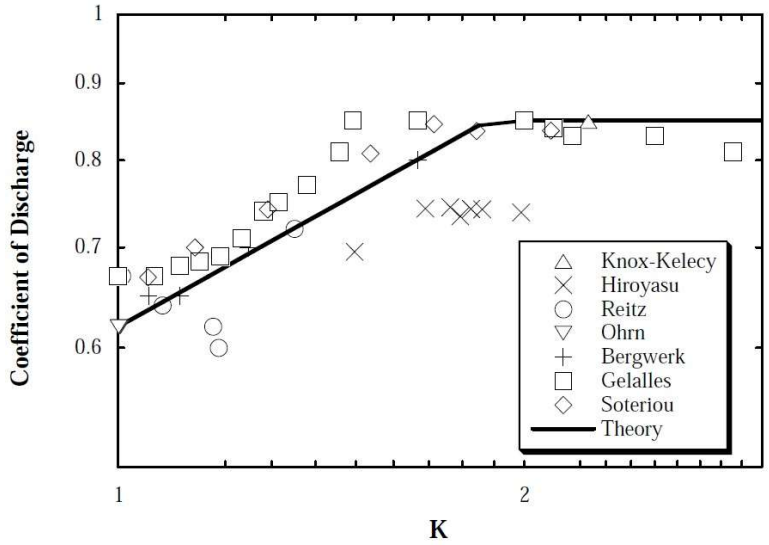

Fig. 2.6. Compilation of experimental nozzle discharge coefficient. Data are plotted on log–log axes. Schmidt and Corradini [5]

The effect of rounding at the inlet increases the coefficient of discharge. Nurik [9] also observed that as K decreases the value of C_d suddenly decreases due to hydraulic flip phenomena, which is also confirmed by Rietz [22]. However, super-cavitation has been observed instead of hydraulic flip in real scale nozzle with realistic operating conditions. The super-cavitation leads to a choked flow condition in which an almost constant mass flow rate is observed with changes in pressure difference.

2.3.2 Multi-dimensional modelling of cavitation flow

The one-dimensional model is preferably good to predict the discharge coefficient with a sharp inlet nozzle but does not give much detail about the internal flow behaviour of the cavitation phenomena. An extensive multi-dimensional numerical model is required to gather information about flow parameters within the nozzle as well as at the outlet of the nozzle, which can later be used to model spray characteristics. Many researchers proposed two-phase numerical models for cavitation flow. These models are capable to calculate the temporal behaviour of cavitating flow with the real-size nozzle geometry, which is fairly expensive with the experiments

2.3.2.1Bubble Dynamics

Fundamentally, cavitation is the phenomenon in which the bubbles grow when the local pressure is lower than the vapour pressure and collapse if the local pressure is more than the vapour pressure. One of the oldest models for bubble growth and collapse was developed by Rayleigh [23]. He considered a spherical liquid bubble with an initial radius of R_0, with an empty surrounding. The pressure at the cavity wall was zero and the pressure at a distance of infinity was a constant, P_∞. The bubble would collapse in time, t is given by:

$$t = 0.915\, R_0 \sqrt{\frac{\rho}{P_\infty}} \tag{2.3}$$

According to this model, when the cavity collapses, the velocity at the wall will reach infinity. Rayleigh [23] recalculated bubble collapse and limited the collapse velocity. Plesset[24] expanded this equation and include vapour pressure, which is also referred to as Linear Rayleigh Equation or simplified Rayleigh Plesset (RP) equation.

$$R = \sqrt{\left(\frac{2}{3}\frac{|P_v - P_\infty|}{\rho}\right)} \tag{2.4}$$

Later Plesset [24] includes surface tension and vapour pressure effect. This is generally referred to the Rayleigh-Plesset (RP) bubble dynamic equation.

$$R\frac{d^2R}{dt^2} + \frac{3}{2}\left(\frac{dR}{dt}\right)^2 + \frac{4\mu}{R}\frac{dR}{dt} + \frac{2\sigma}{\rho R} = \frac{P_b - P_\infty}{\rho} \tag{2.5}$$

Where R is the bubble radius, $\frac{dR}{dt}$is the bubble wall velocity, σ is the surface tension and P_v is the vapour pressure. The bubble dynamic equation proposed by the other researcher is listed in Table 2.2. Although a reduced version of the Rayleigh-Plesset (RP) equation is extensively used in cavitation modelling, notably with the mixture, volume of fluid (VOF), and Eulerian-Eulerian multi-phase approaches.

Table 2.2 Different Forms of Bubble dynamic equation

Author	**Equation**	**Remarks**
Knapp et al. [25]	$P = P_v - \frac{2\sigma}{R} + \frac{NT}{R^3}$	Include the effect of Ideal gas in the cavity. It is useful to predict cavitation inception.
Kato et al. [26]	$\frac{\partial T}{\partial t} + \frac{dR}{dt}\left(\frac{R}{r}\right)^2\frac{\partial T}{\partial t} = \alpha\left(\frac{\partial^2 T}{\partial r^2} + \frac{2}{r}\frac{\partial T}{\partial r}\right)$	This model includes thermal & inertial effects in bubble collapse.

2.3.2.2 Cavitation modelling

The classification of multi-dimensional cavitation modelling is not easy, broadly it can be categorised into two groups (i) Continuum models and (ii) Interface tracking models. Interface capture is a more promising technique, in which the liquid and vapour phase is treated separately. There are individual equations for continuity and momentum that have been solved for each phase, which required more computational time. Rider and Kothe [27] estimated that interface tracking methods required six times the computational cost of the continuum model. In the continuum model, the two phases are considered to be the same fluid. Often, liquid viscosity, surface tension and relative velocity are neglected, and the pressure of the mixture is assumed to be the saturation pressure. The continuum method is a more convenient way of modelling cavitation.

(a) Single Fluid model

The Volume of Fluid (VOF) & Mixture multiphase model consists similar governing equation by considering both phases simultaneously. The vapour fraction conservation equation estimates the phase change process in the mixture model. The VOF method comprises a secondary equation of volume fraction, apart from Navier-Strokes equations and turbulence model equation. The summation of the volume fraction of two phases is equal to unity and thus satisfied the continuity equation. This model was originally proposed by Hirt and Nichols [28] and a transport equation based on liquid volume fraction can be given as:

$$\frac{\partial(\alpha_l \rho_l)}{\partial t} + \nabla \cdot (\alpha_l \rho_l U) = 0 \qquad (2.6)$$

Where U, α_l and ρ_l are the mixture velocity, volume fraction and density of liquid respectively. The VOF required a very fine mesh to capture the interface; therefore, the applications of this model for cavitation flow in fuel nozzles are still limited.

(b) Barotropic model

If the change in the fluid density is considered to be the only function of pressure difference, i.e. ρ=ρ(p), known as Barotropic flow. It implies that the bubble will immediately alter in volume in a two-phase cavitation flow with a modest pressure difference. Different versions of Barotropic models have been proposed by Kubota et al. [29], Delannoy and Kueny et al. [30], Chen and Heister [31], Avva et al. [32], and Schmidt et al. [33].

One of the initial cavitation models proposed by Kubota et al. [29] considers cavitation as a cluster of small bubbles, of identical size and uniformly distributed. He has specified the bubble number density & the initial bubble radius. This model is reasonable for large scale with low Mach number cavitation flow. Delannay and Kueny [30] assumed that the density is a

function of pressure (Barotropic flow) and all the phases are in thermodynamic equilibrium (HEM-Homogeneous Equilibrium Model) at all times. They solved continuity and Euler's equation (i.e. Navier-Stroke equation without viscous diffusion term) and simulated water flow through the venturi. In the intermediate phase (Liquid vapour mixture), the density was changed with pressure following a sine curve. They also conclude that in the absence of interphase, it could be considered an incompressible flow. They achieved reasonably good qualitative results, but deviate from quantitative results from the experiments. Later Chen and Heister [31] excluded the idea of one-to-one mapping of density and pressure and argued that the pressure field should be related to the density history. Because of the consideration of a time effect, density and pressure are not connected by an equation of state. They came up with a relation for the pressure of a cloud of tiny bubbles on the assumption that there were a set number of bubbles per unit mass. However, their methodology is not appropriate for small-scale applications like fuel injector flow. Avva et al. [32] proposed an enthalpy-based model and used an energy equation. The results obtained with this model are reasonably matched with experimental data, but they reported problems with the model's stability hence limited to very low upstream pressure conditions. Schmidt et al. [33] proposed a compressible pseudo-density model for cavitation flow. Their model considers the compressibility of both pure phases, which allows the wave motion in the fluid. They used mass, momentum balance equation and algebraic equation of state for closer hydrodynamic equations. The equation of state was derived from the enthalpy transport equation. This model is preferable for high-pressure fuel injector flow. Schmidt's barotropic Homogeneous Equilibrium Model (HEM) has been adopted by other researchers. It has been implemented in OpenFOAM®[35], which is utilized by Salvador et al.[34]. However, Schmidt et al. [33] & Salvador et al. [34] both have neglected the turbulence effect. They considered that with a very small length scale, cavitation overwhelms the turbulent effect. Reitz et al. [36] include turbulence with HEM and implemented it in KIVA-3V [37].

(c) Mass transport model

The mass transport model also referred to as the Baroclinic model, used the equation of state in combination with a transport equation for liquid and gas volume fractions. A mass transport equation includes a cavitation source term. This model is more accurate to find the physical details of the cavitation phenomena and modelling the detachment of cavity bubbles. There are various mass transport models which has been proposed by a researcher with different source term i.e Merkle et al. [38], Kunz et al. [39], Schnerr and Sauer [40], Singhal et al.

[41], Zwart et al. [42]. To estimate the phase change between liquid and vapour with this model a source term is required in the mass transport equation.

$$\frac{\partial(\alpha_l \rho_l)}{\partial t} + \nabla \cdot (\alpha_l \rho_l U) = R_c + R_e \tag{2.7}$$

Where R_c and R_e are the rates of mass transfer source terms for condensation and evaporation, respectively. U, α_l and ρ_l is the mixture velocity, volume fraction and density of liquid respectively. If there is no mass transfer between phases, RHS is zero, which is the transport equation for the Volume of Fluid (VOF) model.

Merkle et al. [38] and Kunz et al. [39] proposed a pressure-based model for the condensation and evaporation rate to take into account the mass transfer between the two phases. In their source term equation, only the liquid phase contributes to vaporization, therefore, only α_l has been seen. In both models' presence of non-condensable gases and turbulence was measured, however, surface tension and the viscous effect are not considered. These models' main drawback is the large variety of tuning parameters that depend on the different sorts of applications. Schnerr-Sauer [40] proposed a simplified VOF or dispersed VOF and implement Linear Rayleigh Equation to calculate the mass transfer rate. Surface tension and non-condensable gases were not taken into account in this model. Singhal et al. [41] developed a full cavitation model based on Equal Velocity and Equal Temperature (EVET) based on bubble dynamics. They were considered non-condensable gas, which was dissolved and present in the liquid. They included the surface tension(σ) and turbulent kinetic energy (k) in the source term equations. To calculate the overall interface mass transfer rate per unit volume, Zwart et al. [42] assume a uniform bubble size. Their model was based on the linear Rayleigh equation, and they also ignore the presence of non-condensable gas. The mass transfer source terms for condensation and evaporation are listed in Table 2.3.

(d) Two-fluid model

In the two-fluid model, liquid and gas treat separately and the governing equations are solved for both phases. This model can be divided into two groups of approaches: i.e. Euleriaun-Eulerian approach & the Eulerian-Lagrangian approach. The Eulerian-Eulerian approach considers liquid and gas phases in the Eulerian frame of reference. Yuan and Schnerr[43] implemented this approach with CICSAM (compressive interface capturing scheme for arbitrary meshes) method for interface capturing. They consider all three phases' i.e. non-condensable gas, vapour and liquid. Alajbegovic et al. [44] solved a set of mass, momentum, and turbulence equations for each phase of cavitation by treating it as a single mixture with the Linear Rayleigh Equation. They initially predicted a constant bubble number density, but

later they updated the model to take the vapour volume fraction into account. Battistoni et al. [45] implemented his model in AVL Fire®[46]which is similar to that of Alajbegovic et al. [44].

Table 2.3 Different mass transfer source terms for condensation and evaporation

Authors	**Source term for Evaporation ($P_L < P_V$) and Condensation rate ($P_V < P_L$)**
Merkle et al. [38]	$R_e = C_{dest} \frac{\alpha_l \rho_l \min[0, P_l - P_v]}{t_\infty \rho_v (0.5 \rho_l U_\infty^2)}$, ($C_{dest}$=1) $R_c = C_{prod} \frac{(1-\alpha_l) \max[0, P_l - P_v]}{t_\infty \rho_v (0.5 \rho_l U_\infty^2)}$, ($C_{prod}$=80)
Kunz et al. [39]	$R_e = C_v \frac{\alpha_l \rho_v \min[0, P_l - P_v]}{t_\infty \rho_v (0.5 \rho_l U_\infty^2)}$, ($C_v$=100) $R_c = C_c \frac{(1-\alpha_l)\alpha^2 \rho_v}{t_\infty}$, ($C_c$=100)
Schnerr-Sauer [40]	$R_e = -C_v \frac{3\rho_l \rho_v}{\rho_m} \frac{\alpha_l (1-\alpha_l)}{R_b} sgn(P_l - P_v) \sqrt{\frac{2\lvert P_l - P_v \rvert}{3\rho_l}}$. $R_c = C_c \frac{3\rho_l \rho_v}{\rho_m} \frac{\alpha_l (1-\alpha_l)}{R_b} sgn(P_v - P_l) \sqrt{\frac{2\lvert P_l - P_v \rvert}{3\rho_l}}$.
Singhal et al. [41]	$R_e = C_e \frac{\sqrt{k}}{\sigma} \rho_l \rho_v \left[\frac{2(P_v - P_l)}{\rho_l}\right]^{0.5} - \left(1 - f_v - f_g\right)$, ($C_e$=0.02) $R_c = C_c \frac{\sqrt{k}}{\sigma} \rho_l \rho_v \left[\frac{2(P_v - P_l)}{\rho_l}\right]^{0.5} f_v$, ($C_c$=0.01)
Zwart et al. [42]	$R_e = F_{vap} \frac{3\alpha_{nuc} \rho_v (1-\alpha_v)}{R_b} \sqrt{\frac{2\lvert P_l - P_v \rvert}{3\rho_l}}$, ($F_{vap}$=50) $R_c = F_{con} \frac{3 n_0 \rho_v}{R_b} \sqrt{\frac{2\lvert P_l - P_v \rvert}{3\rho_l}}$, ($F_{con}$=0.01)

They used two different methods for the treatment of bubble number density. (I) Mono-dispersed: All bubbles consider the same in size, (II) Poly-dispersed: Bubbles are of variable size. They observe that the Mono-dispersed approach is preferable, as it requires less computational time without compromising accuracy. The poly-dispersed approach is more suitable to study cavitation erosion due to bubble collapse.

The liquid is viewed as a continuum or carrier phase in the Eulerian frame of reference and the vapour bubbles are viewed as discrete or dispersed phases in the Lagrangian frame of reference in the Eulerian-Lagrangian approach. When one of the two phases has a low volumetric concentration or is naturally distributed, this method is preferred. Giannadakis et al. [47] developed the Eulerian-Lagrangian model to simulate cavitation in a fuel injector nozzle. The model takes into account interactions between bubbles, bubble expansion and contraction, turbulent bubble dispersion, and hydrodynamic disintegration. The model was validated with the experimental results of Arcoumaniset al. [13] of real size

nozzle. Sou et al. [48] also used the Eulerian-Lagrangian approach and coupled it with the Rayleigh-Plesset equation. They simulated with a Large Eddy Simulation (LES) turbulent model and validate results with the in-house experiment of large size nozzle with a rectangular cross-section.

Due to significant improvements in computational processors, the use of commercial CFD tools increases in recent times, which allows an understanding of the hydrodynamic behaviour of the cavitation flow in detail. There are different commercial tools are available particularly FLUENT, CONVERGE, AVL-Fire, and Open Foam reported by various researchers. It is also equally important to validate the results obtained from a new model or method implemented in CFD software with experimental data. Experimental work published by Winklhofer et al. [14] is mostly used for validation due to very comprehensive information in terms of quantitative as well as qualitative results. Mohan et al. [49], Saha et al. [50], He et al. [51], Rojas et al. [52], Zhao et al. [53], and Payri et al. [54] validate their model or methods with Winklhofer's experimental data obtained for two-dimensional throttle geometry. A detailed summary of the work carried out in different CFD software by the various researchers is listed in Table 2.4.

2.4 EFFECT OF CAVITATION FLOW ON SPRAY CHARACTERISTICS

Reitz [64,65] elaborates the fuel atomization process in two steps: near nozzle primary break-up and downstream secondary breakup, shown in Fig. 2.7. Liquid fuel comes out in the form of continuous flow up to a finite distance from the nozzle exit, beyond which the primary break-up starts due to flow instability, further breakup of droplets into smaller droplets referred to as a secondary breakup. The internal flow strongly influences the spray characteristics reported by various researchers. Although the effect of cavitation on the droplet size distribution, spray angle etc is still not satisfactorily analysed.

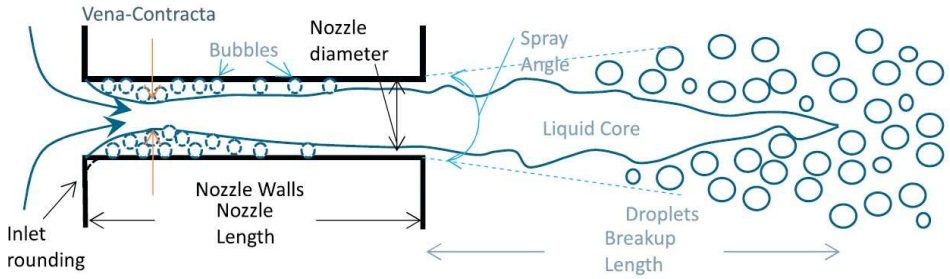

Fig. 2.7 Sketch of the atomization processes of liquid fuel injected from a nozzle, Reitz [64]

Huh and Gosman [66] proposed a phenomenological or one-dimensional model. The cavitation inside the nozzle hole is attributed to turbulent fluctuation at the exit flow being the source of perturbation to the free surface.

Table 2.4 Summary of the work carried out in different CFD tool by the various researchers

Author	Operating pressure, Nozzle dimension	CFD tool	Work detail
R. Payri et al. [55]	P_{inj}=1000 bar, P_{back}=80 bar	ANSYS-Fluent	Compared cylindrical & conical nozzle geometry for cavitation
S. Som et al. [56]	D=0.169 mm P_{inj}=800-1600 bar, P_{back}=1bar	ANSYS-Fluent	Injection pressure, needle lift position and fuel type were analyzed for inner nozzle cavitation flow
Vijayakumar et al. [57]	D=0.169mm, γ=120º P_{inj}=1100 & 1300bar, P_{back}=30bar	ANSYS-Fluent (SS, k-ε)	Calculated C_d for Diesel and blend of Diethyl ether fuels to study the cavitation flow.
Battistoni et al. [58]	D=0.5mm & L=2.5mm P_{inj}=10.6 bar P_{back}=0.87bar	CONVERGE & AVL-Fire	Compared the homogenous mixture model+VOF(implement in CONVERGE) with the multi-fluid non-homogenous model (implement on AVL-Fire) to investigate the cavitation flow.
Battistoni et al. [59]	D_i=0.145mm, D_o=0.13mm, L=1mm P_{inj}=780bar, P_{back}=20bar	CONVERGE (VOF, HRM, RANS)	Compared mass flow rate with available experimental measurement & the effects of needle off-axis motion during the injection event has been studied
Salvador et al. [60,61]	D_{mid}=0.125, D_o=0.156,0.17,0.18mm, L=0.57mm P_{inj}=400bar, P_{back}= 10 to 250 bar	OpenFOAM (HEM, RANS)	Discharge coefficient (C_d), area coefficient (C_a) and velocity coefficient (C_v) is estimated with different convergence-divergence levels to understand the cavitation flow.
Yu et al. [62]	D_i-D_m-D_o=0.155-0.165-0.162mm P_{inj}=1100,700,300 bar, P_{back}=40bar	OpenFOAM (VOF, SS, LES)	Calculate mass flow rates, momentum fluxes, effective injection velocity, and discharge coefficient while taking compressibility into account for various injection situations.
Ahmed et al. [63]	Square hole of 1.94mm P_{inj}=22-28 bar	OpenFOAM (VOF, SS, LES)	Considered non-condensable and uses the inter-phase capturing method.

They correlate the spray angle with turbulence quantities at the nozzle outlet. They also extend their work and correlate spray break-up with turbulence but do not include the cavitation effect. Arai et al. [67,68,69] found that the spray characteristics change dramatically and the atomization can be enhanced with the presence of cavitation bubbles from the inlet to the exit of a nozzle. The collapse of the cavitation bubble promotes the liquid jet breakup. The geometry of the nozzle and the pressure boundary conditions affect the cavitation's structure. If the length of the nozzle is long enough, the cavitation bubble does not reach the nozzle exit. In this case, He and Ruiz [70] found that cavitation still influences the downstream flow field by adding turbulent intensity within the flow. Arcoumanis et al. [71] proposed a spray model considering the effect of upstream conditions i.e. transient fuel injection behaviour, turbulence and nozzle cavitation. The model includes several constants to estimate the nozzle discharge and primary breakup. This model offers an important step in the coupling of nozzle flow to the downstream spray prediction. In a similar topic, Sarre et al. [72] produced a model for a multidimensional spray with the help of cavitating and non-cavitating nozzle flow regimes maps.

2.4.1 Cavitation coupled spray model

Comprehensive multidimensional cavitation coupled spray model has evolved recently, due to the requirement of high computational cost. There are two different approaches researchers are following. The first one is the two-step approach, where two separate calculations using the Eulerian model to simulate cavitation inside nozzle flow and the Lagrangian approach for the outside injector for the spray region. In this method, discrete particles are superimposed on the continuous gas phase. Reitz [73] proposed a linear phenomenological or one-dimensional model in which, liquid droplets consider ‘blobs’ are injected at the outlet of the nozzle and are applied to account for the primary breakup. The model’s consistency at near nozzle flow is poor due to an inherently weak connection to the inner nozzle flow. Berge et al. [74, 75], Som et al. [76, 77, 78] and Wang et al. [79] work to predict the near nozzle flow by considering the effect of nozzle turbulence & cavitation on the primary breakup. Berge et al. [74] developed a methodology to couple spray and internal nozzle flow at AVL and applied it within the framework of FIRE CFD code. They adopt a two-fluid model for cavitation flow and a Discrete Droplet Model (DDM) for spray simulation. Som et al. [78] implemented KH-ACT (Kelvin Helmholtz-Aerodynamic Cavitation Turbulence) model in CONVERGE®[80] to simulate spray characteristics of diesel and bio-diesel and compared it with data from Sandia national laboratory. Battistoni et al. [81] reported similar work by using the result of the first

computing step, mapped at the nozzle exit area, for the initialization of the primary breakup model.

In the second approach, both liquid and vapour are considered in the continuum phase and the conservation laws are solved under Eulerian flow assumptions. This required grid refinement up to the sub-micron level to detect droplets without injecting any discrete particles. Lebas et al. [82] use DNS (Direct Numerical Simulation) and Oley et al. [83] conducting simulation with LES (Large Eddy Simulation). This approach is also termed as 'quasi-DNS', however, its application is limited due to its high computation cost. Salvador F.J [84] proposed Σ-Y Eulerian coupled model implemented in CONVERGE® software. This model has been validated with the results of Spray A and Spray-C from the Engine Combustion Network (ECN). Spray A is a non-cavitating nozzle with a high k-factor and a convergent diameter of 90 μm. In contrast, Spray C is a cavitating nozzle with a constant diameter of 200 μm and a k-factor of zero. The validated models are used to examine the flow conditions and spray characteristics at the nozzle outlet for the elliptical nozzles. This includes factors such as mass flow, momentum flux, liquid and vapour fractions, radial and axial velocity profiles, as well as spray features such as spray angle, air entrainment, and spray tip penetration. Despite the various methods reported recently, a rigorous and realistic method to simulate both the internal cavitation flow and spray formation is yet to be reported. In this case, experimental work can be useful to understand the effect of cavitation flow on the spray characteristics.

2.4.2Experimental study on cavitation-induced spray breakup

Sou et al. [85, 86], Suh and Lee [87], Bicer et al. [88], and Abderrezzak [89] conducted a thorough study to examine the impact of cavitation on spray characteristics using a 2D transparent acrylic nozzle geometry. They employed nozzles of different length-to-width ratios. The nozzle geometry has a significant effect on spray characteristics i.e. spray cone angle and ligament formation. They also observed that super-cavitation, where vapour bubbles are swept outside the nozzle exit, had a considerable effect on the atomization characteristics. Most of the experimental study has been carried out with the transparent 2D nozzle so that they could allow visualization of cavitation inside the nozzle. There is still a considerable lack of information on the influence of cavitation with the use of real-size 3D nozzles on spray formation. Payri et al. [90, 91, 92] and Desantes et al. [93] conduct experimental and numerical studies to measure the effect of cavitation on the velocity, mass flux and momentum flux at the exit of the bi-orifice nozzle. For this study, they have used two different nozzles (I) Cylindrical and (II) Conical. They concluded that the cavitation produces

a substantial increase in a spray cone angle. The shear stress between the nozzle wall & fluid will decrease due to the presence of cavitation. However, there is limited visualization information regarding the development of cavitation flow. The captured images are not very clear to distinguish the different regimes of cavitation and their effect on liquid atomization. Abbasiasl T. et al. [94] used a micro-scale nozzle to visualize cavitation, and the effect of cavitation on spray is investigated in terms of cone angle, droplet size distribution and droplet velocity distribution. They observed that the spray angle improved during developing cavitation and super-cavitation regimes but drop significantly during the cavitation flip, as shown in Fig.2.8. Hwang J. [95] provides an in-depth analysis of the interaction of cavitation with sprays in high-pressure diesel injection systems. The author discusses various experimental techniques used to study cavitation in diesel fuel injection systems, such as high-speed imaging, X-ray radiography, and acoustic measurements. The author also describes various mathematical models used to simulate cavitation in fuel injection systems, including empirical models, numerical models, and analytical models.

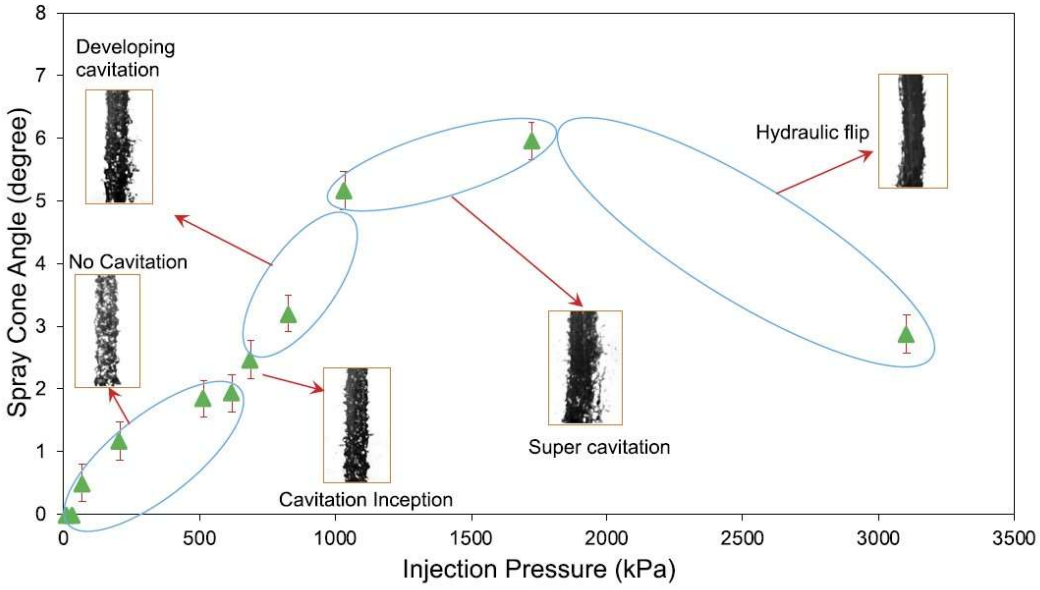

Fig.2.8 Spray cone angle with different cavitation flow pattern map, Abbasiasl T. et al. [94]

2.5 VORTEX INDUCED CAVITATION

Recent research has identified two different types of cavitation, which have been further defined as geometry-induced cavitation and vortex-induced cavitation or string-type cavitation as shown in Fig. 2.9. It is believed that cavitation bubbles can be found within the low-pressure region of a highly-organized, large-scale vortex structure that develops in regions with high vorticity. The phenomenon of geometric-induced cavitation occurs at sharp corners where the pressure is lower than the vapor pressure of the liquid. On the other hand,

string or vortex cavitation occurs in the bulk of the liquid of sac or min sac-type nozzles, where large-scale vortices can be formed due to the available volume relative to the nozzle geometry. Gavaises M. et al [96] define the string cavitation using 6 holes transparent cylindrical and tapered nozzle (d_{in}= 2.8 mm, d_{out}=2.5mm, L=15mm). It is found that the String cavitation emerges in regions where large-scale vortices form, originating from either pre-existing geometric cavitation sites or trapped air downstream of the hole exit. Small variations in the shape of the needle and needle eccentricity have been found to significantly affect the cavitation strings.

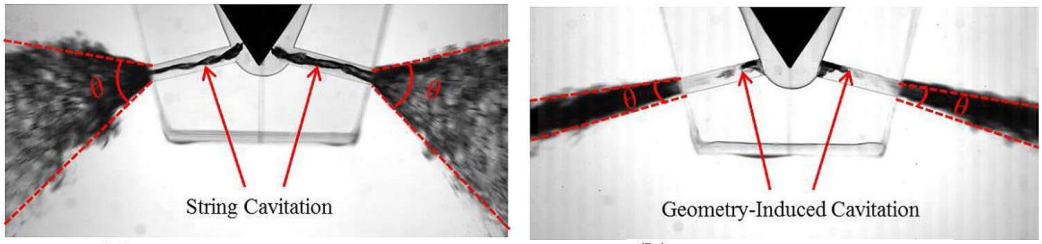

(a) P_{inj}=0.4 MPa, P_{amb}=0.1 MPa **(b)** P_{inj}=0.2 MPa, P_{amb}=0.1 MPa

Fig 2.9 Two types of cavitation patterns obtained by shadow photography Cao T et al. [97]

The study by Cao T et al. [97] aimed to investigate the effect of fuel temperature and different cavitation patterns on the development of cavitation inside diesel injector nozzles. The experiments were conducted using a transparent two-hole injector nozzle (d_{in}=2.1 mm, d_{out}=2mm, L=10 mm) and shadow photography. They observe String-type cavitation at 1 mm of needle lift and Sheet-type cavitation caused by the geometry of the near-wall region occurs as the needle lift to 2 mm. The results showed that the string-type cavitation was more sensitive to fuel temperature and had a significant impact on the spray angle and penetration, while the sheet-type cavitation had a minor effect on the spray characteristics and was less sensitive to the fuel temperature.

Prasetya R et al. [98] and Nurcholik S D et al. [99] explore the three-dimensional structure of the string cavitation by using an enlarged three-hole cylindrical mini-sac cylindrical nozzle (d=2 mm, L=8 mm). They used tomographic-stereo particle image velocimetry (TSPIV) to obtain flow structure under different needle lift conditions (Z/D=0.5, 1 & 3). When needle lift is high (Z/D=3) the vertical velocity gradient is low, which makes it harder to form string cavitation. At Z/D=1, twin string cavitation swirling flow was observed. At a low needle lift ratio of Z/D = 0.5, a single stable string cavitation with a larger diameter is produced by a steady swirling flow upstream of an orifice. This swirling flow creates a steady spiral flow in the orifice and a hollow-cone spray, resulting in a notable increase in spray angle. Guan W et al. [100] performed experimental and numerical studies to characterise

string-type cavitation in real-size tapered nozzles (d_{in}=0.33 mm, d_{out}= 0.26 mm, L=1.84 mm). The diesel fuel was used to inject at an injection pressure of 60 MPa. They performed numerical simulations by using a three-phase VOF model with the SS cavitation model in the ANSYS-Fluent platform. The results show that the vortex flow can significantly alter the cavitation shape and length, while the cavity intensity is relatively insensitive to the vortex flow. According to the analysis based on the equation for vorticity transport, the main factor in the creation and growth of string cavitation is the stretching of the vortex. The impact of the dilatation term, which is connected to the compressibility of the fluid, is of lesser importance, followed by the effect of the baroclinic torque term on the distribution of vorticity. Wei Y et al [101] also used real size tapered shape nozzle to understand cavitation flow and near-field spray under multiple injections. The author investigated the impact of multiple injections on the internal flow and spray characteristics in the vicinity of the nozzle, specifically focusing on how needle valve throttling and pressure fluctuations at the nozzle inlet contributed to these effects. The study found that the spray cone angle and the spray area ratio increase slowly in the form of "boot-shaped", followed by a sudden increase during the main injection. The string cavitation is observed when the position of the needle valve shifts and the spray cone angle increases suddenly. Kumar A et al. [102] performed a numerical study by using 20 times scaled-up mini-sac type six-hole injector nozzle (d=3.5mm). They implemented a mixture multiphase model with a Zwart-Gerber-Belamri (ZGB) cavitation model in ANSYS-Fluent. They successfully captured the vortices structure by using the RANS turbulence model.According to the analysis, two primary types of vortex structures were observed.

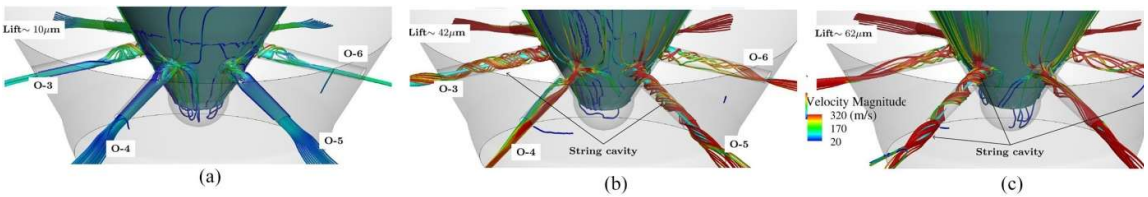

Fig.2.10 String cavitation at selected needle lift during the SOI Gavaises M. et al [103]

The first type of structure, referred to as "hole-to-hole" connecting vortices, is formed by connecting two neighbouring holes. The second type of structure, characterized by double counter-rotating vortices, originated from the needle wall and entered the injector hole opposite to it. Gavaises M. et al [103] present a numerical investigation of fuel dribbling and wall-wetting phenomena in a multi-hole diesel injector nozzle. The simulations were carried out using commercial CFD software ANSYS Fluent, with a two-phase Eulerian-Lagrangian approach shown in Fig. 2.10. The movement of air is modelled using an extra equation for

transport, which is linked with the VOF interface capturing technique to accurately represent the atomization process near the nozzle, and to capture the effects of the liquid spray on the nozzle walls. The model incorporates a pre-defined movement of the needle inside the VCO nozzle along both the axial and eccentric directions, utilizing an immersed boundary technique called the IBM. It is observed that the vortex or string cavities are created from the needle surface to the orifice exit, while small droplets and ligaments are formed near the nozzle exit region. The swirling flows inside the orifices are intensified due to the needle's eccentric motion, which plays a key role in breaking up the injected liquid jet into ligaments and directing them backwards towards the external wall of the injector. The study reveals that wall-wetting effects are more noticeable when the valve is closing and fuel injection is occurring in subsequent events. This is due to the presence of residual gases trapped in the nozzle, which facilitate the complete atomization of the injected fluid.

2.6 CAVITATION ASSISTED BIODIESEL PRODUCTION

Hydrodynamic cavitation (HC) is an advanced technique for enhancing the transesterification process in biodiesel production. It involves the generation, growth, and collapse of vapor bubbles in a liquid due to pressure variations. The rapid collapse of these bubbles' releases intense localized energy, leading to enhanced mixing, mass transfer, and reaction kinetics, making biodiesel production more efficient compared to conventional methods. Hydrodynamic cavitation (HC) offers significant advantages over conventional stirrer-based biodiesel production by enhancing mass transfer and reaction kinetics through intense localized energy release from collapsing cavitation bubbles. This method can achieve improved results, yielding more than 90% biodiesel within a processing time of 15–30 minutes [104].

The efficiency of biodiesel production using hydrodynamic cavitation (HC) technology is influenced by various factors, such as reactor type, oil-to-alcohol molar ratio, catalyst type and concentration, temperature, and reaction duration. Among different cavitation devices used for converting vegetable oils into biodiesel, the multi-hole orifice has been recognized as the most effective, achieving a 99% biodiesel yield within just 15 minutes of processing [105]. Higher biodiesel yield can be achieved for a higher number of holes. Another crucial factor influencing the transesterification process is the oil-to-alcohol molar ratio. Typically, increasing this ratio up to an optimal level enhances biodiesel production while reducing the required reaction time. For instance, raising the molar ratio from 1:4 to 1:6 led to an increase in biodiesel yield from 45.2% to 98.1% within a treatment time of just 15 minutes [106]. In addition to the molar ratio, the amount of catalyst used also plays a significant role in the

transesterification process. Increasing the catalyst concentration, such as sodium hydroxide (NaOH) or potassium hydroxide (KOH), from 1 to 2 wt% can enhance biodiesel production. However, exceeding the optimal catalyst dosage can negatively impact the transesterification yield due to soap formation, as excess NaOH or KOH reacts with free fatty acids present in the system. It concluded that the biodiesel production using hydrodynamic cavitation provides opportunities to make the production of biodiesel more affordable, quick, environment friendly and sustainable.

2.7 RESEARCH GAP

As summarised in the literature review, a lot of researchers attempted to investigate the cavitation process in fuel injector nozzles using both experimental and numerical methodologies, with diesel as the fuel. There is a substantial body of literature on the cavitation phenomenon in fuel injector nozzles. However, relatively little research has been published on cavitation-induced primary breakup. A lot has been learned from experimental experiments, but the pattern of the two-phase mixture remains unclear. It is also identified that the fuel jet break-up process during the early phases of droplet generation in injectors is still not fully understood. The cavitation phenomena are still being studied for diesel fuel in fuel injectors, with the goal of better understanding what happens when biodiesel is used as fuel in an internal combustion engine. The current research aims to investigate the effect of various factors on the internal flow of a fuel injector nozzle and its spray characteristics using diesel and blends of biodiesel. The research also proposed a two-step coupling method to incorporate the influence of cavitation on primary liquid spray breakup, which leads to spray atomization in secondary breakup utilising numerical techniques.

2.8 RESERCH OBJECTIVES

- This research proposes the detailed assessment of an existing two-phase numerical model to study the cavitation phenomena inside the fuel injector nozzle.
- It is proposed to validate the results with existing experimental data available in the literature for diesel as fuel and explore the limitations of the numerical model.
- It is proposed to calculate the flow parameter at the outlet of the nozzle in both cavitation and non-cavitation conditions. These results are used to assign the initial condition for spray simulations as a part of the two-step coupling method.
- The hydrodynamic behaviour and size of cavitation bubbles will be investigated under different operating conditions to develop a cavitation map using experimentation.

- To investigate the spray characteristics of diesel, tallow biodiesel and WCO biodiesel, by incorporating the effect of cavitation.
- The results are assessed and based on that the recommendation for the new fuel injector nozzle design can be proposed for biodiesel.

2.9 EXPECTED OUTCOMES

This research work proposes a numerical model for the development of a fuel injector nozzle using biodiesel as a fuel with a cavitation phenomenon, which could provide a reasonable estimation with different boundary conditions, for better prediction of spray breakup. Therefore, the outcome of the present research work is expected as below:

- A detailed assessment of the existing numerical model to study cavitation phenomena inside the fuel injector nozzle using biodiesel as fuel and evaluate its limitations. A numerical model with suitable modifications and its results will be compared with existing experimental data available in the literature for diesel as fuel to validate the said numerical model.
- A two-step coupling method will help to understand the effect of cavitation on spray characteristics. In the framework of cavitation phenomena, favourable operating conditions and geometrical parameters of the injector nozzle for primary breakup will be identified.
- Finally, a suitable design of fuel injector nozzle will be proposed for biodiesel used in four stroke diesel engines, which is supposed to have better atomization characteristics and improve the performance of the engine.